Ionics (2017) 23:3497–3506
DOI 10.1007/s11581-017-2141-7

ORIGINAL PAPER

Response characteristics of lead-selective membrane sensors based on a newly synthesized quinoxaline derivatives as neutral carrier ionophores

Ayman H. Kamel[1] · **Abeer M. El-Naggar**[1] · **Amina A. A. Argig**[1]

Received: 16 February 2017 / Revised: 30 April 2017 / Accepted: 1 May 2017 / Published online: 7 June 2017

Abstract Novel lead-selective polymeric membrane sensors were prepared based on the use of 2,2′-(quinoxaline-2,3-diyl bis (azanediyl)) dibenzoic acid (sensor I) and *N*′-(3-chloroquinoxalin-2-yl) nicotinohydrazide (sensor II) as novel synthetic neutral carrier ionophores embedded in a plasticized poly(vinyl chloride) (PVC) matrix. The sensors displayed near-Nernstian cationic slope of 35.3 and 37.18 mV/decade over the concentration range 7.0×10^{-6}–1.0×10^{-3} and 4.0×10^{-6}–1.0×10^{-3} M at pH 5 with lower detection limits of 4.7×10^{-6} and 1.8×10^{-6} M for sensors (I) and (II), respectively. The influence of anionic additive on the potentiometric responses of the prepared membrane sensors was studied. The selectivity studies showed high selectivity towards Pb(II) ions over large number of other cations for all the proposed sensors. Formal complex formation constants of the ionophores with Pb(II) and a series of interfering cations have been determined in the organic membrane phase. The formal complex formation constants found are in excellent agreement with those determined by potentiometric selectivity measurements. The sensors were subjected to lead assessment in biological fluid samples either in static and flow-through mode of operations. The results obtained agree fairly well with data obtained by atomic absorption spectrometry (AAS).

✉ Ayman H. Kamel
ahkamel76@sci.asu.edu.eg

[1] Department of Chemistry, Faculty of Science, Ain Shams University, Abbasia, Cairo 11566, Egypt

Keywords Lead · Quinoxaline derivatives · PVC membrane · Potentiometric transducers · Flow-through analysis · Formal complex formation constants

Introduction

Controlling the levels of environmental pollutants in natural waterways and drinkable water has created enhanced attention and high significance in the production of new sensors for the assessment of heavy metals [1]. Heavy metals have been a dangerous and complex problem and have stayed a focus of interest all over the world [2]. Lead is considered as one of the highly toxic chemicals that show dangers on human's health. It has cardiovascular effects, renal disease, neurologic damage, and reproductive toxicity [3]. Continuous exposure to lead causes toxic effects to the brain, blood, nervous system, and reproductive system. In young children, a collection of lead causes brain damage and mental retardation. Lead also has the ability to replace calcium in bone to form sites for long-term release. Assessment of accumulation, deficiency, and concentration of low levels of lead in biological and environmental samples requires sensitive, reproducible and accurate analytical techniques [4, 5].

Several of analytical methods are highly desirable for lead determination but most of these techniques are time consuming, too expensive for most analytical laboratories, and demand the very specific sample preparation [3, 6]. Several analytical techniques have been used to determine lead including gas chromatography [7–11], high-performance liquid chromatography (HPLC) [12–15], mass spectrometry [16–20], and spectrophotometry [21–23]. Electroanalytical methods are the most suitable for direct quantification of many ions and are used in routine analysis in many fields, due to their high sensitivity and selectivity in their responses [24–27]. Among

the electrochemical methods, potentiometric sensors possess wide concentration range, fast analysis time, ability of measurement in colored or turbid solutions, high sensitivity and suitable accuracy, and also cost-effectiveness [28, 29]. In the literature, many attempts have been cited to develop many potentiometric sensors for lead assessment [30].

The development of neutral carrier-based potentiometric sensors offered a possibility of enhancing the selectivity towards lead ions over various interfering cations and decreasing the detection limit. Decades passed since the development of the first plastic membrane with ionophore [31]. Since then a great number of lead ionophores was synthesized and characterized in potentiometric electrodes [32–34]. The main groups of these compounds recognized as lead-selective ionophores are crown ethers [35–37], calixarenes [32, 38–40], 2,6-bis-pyridinecarboximide derivatives [41], Schiff base derivatives [42–44], and dioxamides [45, 46]. Due to environmental restrictions towards distributions of selected heavy metals like lead, the research in the field of synthesis and characterization of compounds as novel lead (II)-selective ionophores is vibrant.

The novelty of the present work depends on the investigation and the use of newly synthesized quinoxaline derivatives as a neutral carrier type ionophore in polymeric membranes. The feasibility of employing the above quinoxaline derivative as carrier for lead is characterized and its potentiometric response in terms of linear range, lower limit of detection, slope, time response, and selectivity over common organic and inorganic cations is described. The sensors were also introduced as detectors in a flow-through manifold for automatic lead quantification. They were also applied for the assessment of lead in biological fluid samples and lead alloy samples using potentiometric determination, standard addition and the calibration curve methods under static and hydrodynamic mode of operations.

Material and methods

Apparatus

All potentiometric measurements were performed at ambient temperature with an Orion digital pH/mV meter (model SA 720), using lead PVC membrane sensors in conjunction with an Orion Ag/AgCl double junction reference electrode (type 90-02) filled with 10% (m/v) KNO_3 solution in the outer compartment and Ross glass pH combination electrode (Orion 81-02) was used for all pH measurements. The potential signals were measured for stirred Pb(II) solutions using the following electrochemical cell: Ag/AgCl/10^{-2} M Pb(II)/membrane/sample test solution/double junction Ag-AgCl reference electrode.

Reagents and chemicals

All reagents used were from analytical grade and double-distilled water was used for all subsequent solution preparations. High molecular weight poly(vinyl chloride) (PVC), dioctyl phthalate (DOP), tetrahydrofuron (THF), tetramethylammonium chloride (TMAC), and potassium tetrakis-[3, 5-bis(trichloromethyl)phenyl]borate (KTClPB) were purchased from Fluka (Ronkonkama, NY). Metal nitrates, chlorides, and sulfate were of the highest purity available. 2,3-Dichloroquinoxaline, anthranilic acid, tridodecylmethylammonium chloride (TDMAC), and isonicotinic hydrazide were purchased from Sigma-Aldrich (St. Louis, MO).

Acetate buffer 10^{-2} M of pH 5 was freshly prepared and the ionic strength was adjusted with 5×10^{-2} M KNO_3. A 10^{-2} M stock solution of $Pb(NO_3)_2$ was freshly prepared. Working solutions (10^{-7}–10^{-2} M) were prepared from nitric acid then accurate dilutions.

Synthesis of the ionophores

To a solution of 2,3-dichloroquinoxaline (1.97 g, 1 mmol) in ethanol (20 mL), the appropriate amine (isonicotinic hydrazide and anthranilic) (1 mmol) was added and the reaction mixture was heated under reflux for 4 h. The solution is then left to cool to room temperature. The precipitate was collected by filtration and re-crystallized from appropriate solvent. A schematic representation for the synthesis pathway is illustrated in Fig. 1.

Membrane preparation and potential measurements

The membranes are generally prepared by incorporating 10 mg of each ionophore with 350 mg of the plasticizer

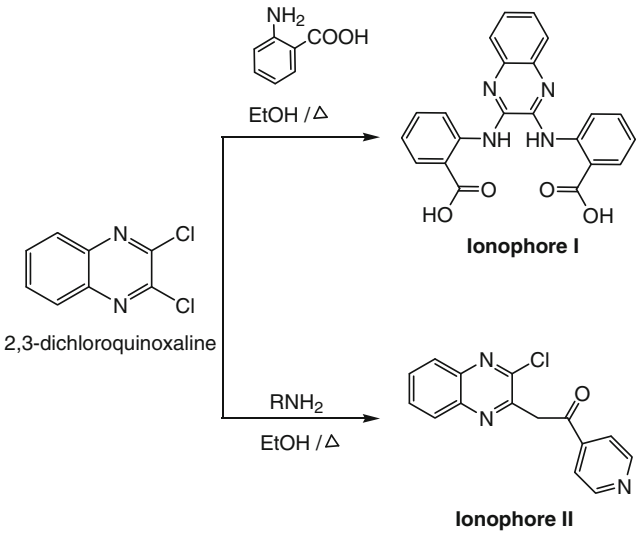

Fig. 1 Schematic route for the synthesis of the ionophores

DOP and 190 mg PVC in PVC with the aid of 4 mL tetrahydrofuran. The solution mixture was poured mixture into a 5-cm Petri-dish and the solvent is allowed to evaporate, leaving a tough flexible membrane with the components trapped in the PVC matrix. Discs of appropriate diameter are cut from the "master membrane" and cemented to the flat end of a PVC tubing using THF. The tube was filled with 10^{-2} M $Pb(NO_3)_2$ as internal solution and a 3-mm-diameter Ag/AgCl-coated wire was used as an internal reference electrode. Sensors were conditioned by soaking in 10^{-2} M aqueous lead ion solutions for 24 h before use and were stored in Pb(II) solutions when not in use.

Sensors were calibrated by their immersion into a 25-mL beaker containing 10 mL of 1.0×10^{-2} M acetate solution of pH 5 in conjunction with an Ag/AgCl double junction reference electrode. An aliquot (0.5–1.0) mL of 10^{-6}–10^{-2} M standard Pb^{+2} solutions were successively added and the potential response of the stirred solutions was measured after stabilization to ±0.2 mV. A calibration was building up by plotting the EMF reading against the logarithm of Pb^{+2} concentrations.

For flow-through measurements, the flow cell used for of Pb^{+2} monitoring was designed to accommodate small sensor size. The membrane solution was prepared as previously mentioned above. The solution was deposited using a microdropper into a hole (3 mm wide) made in the middle of a 5-cm Tygon tube, then the solution was allowed to evaporate. The tube was then inserted into a pipette tip which was closed to prevent leakage of the internal reference solution. This design is to avoid large consumption of the sample and to give high response with short recovery time. The sensor was inserted into the flow injection system and 10^{-2} M acetate buffer, pH 5, was used as a carrier solution at a flow rate of 5.0 mL/min. The electrode was placed at a distance about 30 cm from the injection valve and in a conjunction with a double junction Ag/AgCl reference electrode. The electrode was calibrated by injection of Pb(II) ions standard solutions through a valve loop of about 200 μL volume. After the baseline was reached, the potential signals were recorded using the data. The average potentials at maximum heights were plotted against log [Pb(II)].

Determination of formal stability constants

The formal stability constants between the two ionophores and common transition elements including lead (II) were evaluated as that shown above for ISE measurements, as described in detail in reference [47]. For this purpose, two plasticized PVC membranes (the first one based on (KTClPB) (0.5 wt%), *o*-NPOE (66.1 wt%), and PVC (33.4 wt%)) only and the second one containing the given ionophore (1.73 wt%) and the same amount of (KTClPB) (0.5 wt%), *o*-NPOE (66.1 wt%), and PVC (33.4 wt%) were prepared. A series of membrane discs were then cut and glued with THF/PVC slurry to plasticized PVC tubing. These discs were conditioned over 2 days in 10^{-2} mol L^{-1} solution of appropriate salt [$Cu(NO_3)_2$, $Zn(NO_3)_2$, $Hg(NO_3)_2$, or $Fe(NO_3)_3$]. To determine the stability constants for a given ionophore and a given cation, two cell EMF measurements, one for a membrane without ionophore and then for the two sandwiched membranes were carried out. The sandwiched membrane was made after drying of individual membranes, by attaching of the membrane with ionophore to the ionophore-free membrane. The segmented membrane was then mounted into electrode body (membrane with ionophore facing the sample solution) and immediately immersed into an appropriate salt solution (identical as that used for conditioning of the membrane). The potential was recorded as the mean EMF value over the last minute of a 5-min measurement period. The change in membrane potential values (E_M) were calculated by subtracting the cell potential measured for a membrane without ionophore from the potential when the sandwiched membrane configuration was used. The formation constants were calculated according to Eq. (1) [47].

$$\beta_{IL} = \left(L_T - nR_T \Big/ Z_i\right)^{-n} \exp\left(E_M Z_i F \Big/ R_T\right) \quad (1)$$

where L_T is the concentration of ionophore in the membrane, R_T is the concentration of anionic additives in the membrane, and n is the stoichiometric ratio between Pb(II) and the ionophore (i.e., $n = 1$).

Lead assessment in biological fluids

Aliquots of human serum (~3.0 mL) were transferred to 10 mL polypropylene sample tubes. A 9-mL portion of acetonitrile was added, thoroughly mixed, and left for 5 min before being centrifuged at 1000 rpm. The supernatant liquid was transferred to a 50-mL beaker and then completed to 25 mL by 10^{-2} M acetate buffer at pH 5 and used for batch lead measurements. The lead sensor and reference electrode were immersed to 10 mL of 10^{-2} M acetate buffer (pH 5) after adding successive aliquots of the spiked serum solutions. The potential readings were measured after reaching the equilibrium response. The concentration of Pb^{2+} ions added was calculated using a calibration graph.

Lead quantification in alloys

A 0.3-g portion of a Pb/Sn alloy samples were transferred to a 25-mL beaker. A 5–10-mL aliquot of (1:1) nitric acid was added and the beaker was placed on a hotplate inside a fuming hood until the alloy is completely dissolved. The sample solution was allowed to cool and diluted with 0.01 M acetate buffer (pH 5) to a 25-mL volumetric flask. In 10 mL of the sample, the lead sensor in combination with the reference

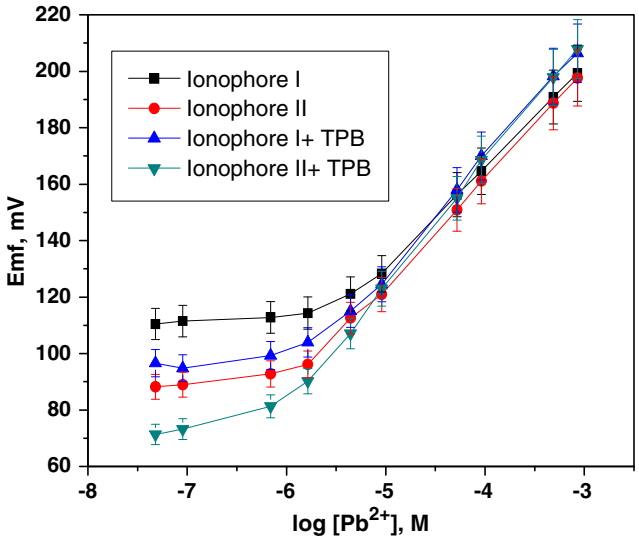

Fig. 2 Calibration plot of sensors based on ionophores (I) and (II) in 0.01 M acetate buffer at pH = 5

electrode was immersed in the solution. The potential readings were measured after reaching the equilibrium response and the concentration of lead ions in the alloy was calculated using the constructed calibration graph.

Results and discussion

Elucidation of ionophores structures

2,2′-(quinoxaline-2,3-diyl bis (azanediyl)) dibenzoic acid (ionophore I) Yield 88%; brown crystals; m.p. >300 °C (EtOH); IR (max/cm^{-1}): 3285, 3225, 3149, 3110 (OH and/or NH), 1687 (C=O) (chelated), 1597, 1570, 1539 (C=N and/or C=C), 745 (δ_{4H}) cm^{-1}; ^{1}H-NMR (400 MHz, DMSO-d$_6$): δ7.10–9.38 (m, 12H, Ar-H), 11.98 (br.s, 2H, NH, exchangeable), 12.47 (br.s, 2H, OH, exchangeable); MS *m/z*: 400 [M$^+$] (2), 299 (9), 267 (10), 256 (20), 254 (38), 246 (28), 239 (10), 137 (16), 111 (16), 98 (40), 85 (24), 77 (28), 57 (83), 43 (100); anal. calcd % for $C_{22}H_{16}N_4O_4$ (400.39): C, 66.00; H, 4.03; N, 13.99; found%: C, 66.02; H, 3.98; N, 13.90.

***N′*-(3-chloroquinoxalin-2-yl) nicotinohydrazide (ionophore II)** Yield 88%; brown crystals. m.p. over 300 °C (EtOH); IR (max/cm^{-1}): 3190, 3147(NH), 3049 (CH_{aryl}),1643 (C=O), 1611 (C=N), 1549, 1504 (C=C), 850 (δ_{2H}), 748 (δ_{4H}) cm^{-1}; ^{1}H-NMR (300 MHz, DMSO-d$_6$): δ7.12–8.82 (m, 8H, Ar-H), 8.26 (br.s, 1H, NH, exchangeable), 11.02 (br.s,1H,NH-CO), MS *m/z*: 300 [M^{+1}] (56), 298 (49), 297 (58); anal. calcd % for $C_{14}H_{10}ClN_5O$ (299.72): C, 56.10; H, 3.36; N, 23.37; found%: C, 56.42; H, 3.66; N, 23.52%.

Sensors characteristics

Two quinoxaline derivatives (Fig. 1) were prepared and examined as novel neutral carriers for Pb(II) ions in PVC matrix membrane sensors. The membrane composition was 34 wt.% PVC, 64 wt.% plasticizer, and 2 wt.% ionophore. Five membrane sensors for each ionophore were prepared and evaluated during 6 months according to IUPAC recommendations [48]. Sensors incorporating ionophores (I) and (II) revealed a strong response towards lead ions. Results of triplicate measurements showed a potentiometric response with near-Nernstian slope of 35.3 ± 0.9 and 37.18 ± 0.3 mV/decade (r^2=0.9997), with linear range 7.0×10^{-6}–1.0×10^{-3} and 4.0×10^{-6}–1.0×10^{-3} M and a detection limit of 4.7×10^{-6} and 1.8×10^{-6} M for sensors incorporating ionophores (I) and (II), respectively. Potentiometric response of these sensors is shown in Fig. 2. Addition of 0.5 wt.% anionic additive (Na-TPB) to ionophores (I) and (II) significantly improved the detection limit from 4.7×10^{-6} to 8.0×10^{-7} M and 1.8×10^{-6} to 6.0×10^{-7} M and increased the calibration slope from 35.3 ± 0.9 to 39.4 ± 1.1 and 37.2 ± 0.3 to 43.9 ± 0.7 mV/decade, respectively. The general response characteristics of

Table 1 Potentiometric response characteristics of Pb(II) membrane-based sensors

Parameters	Sensor I	Sensor I + TPB	Sensor II	Sensor II + TPB
Slope, mV/decade	35.3 ± 0.8	39.4 ± 1.1	37.2 ± 0.7	43.9 ± 0.7
Correlation coefficient, r^2	0.9997	0.9945	0.9982	0.9985
Linear range, M	7.0×10^{-6}–1.0×10^{-3}	1.0×10^{-6}–1.0×10^{-3}	4.0×10^{-6}–1.0×10^{-3}	5.0×10^{-6}–1.0×10^{-3}
Detection limit, M	4.7×10^{-6}	8.0×10^{-7}	1.8×10^{-6}	6.0×10^{-7}
Working range, pH	4.0–6	4.0–6	4.5–6	4.5–6
Response Time, (s)	<20	<20	<20	<20
Life span, (week)	8	8	8	8
Standard deviation, σ_v (mV)	0.9	0.8	1.2	1.1
Accuracy, (%)	99.4	99.3	99.5	98.8
Precision, CV_w (%)	0.8	1.1	0.7	1.2

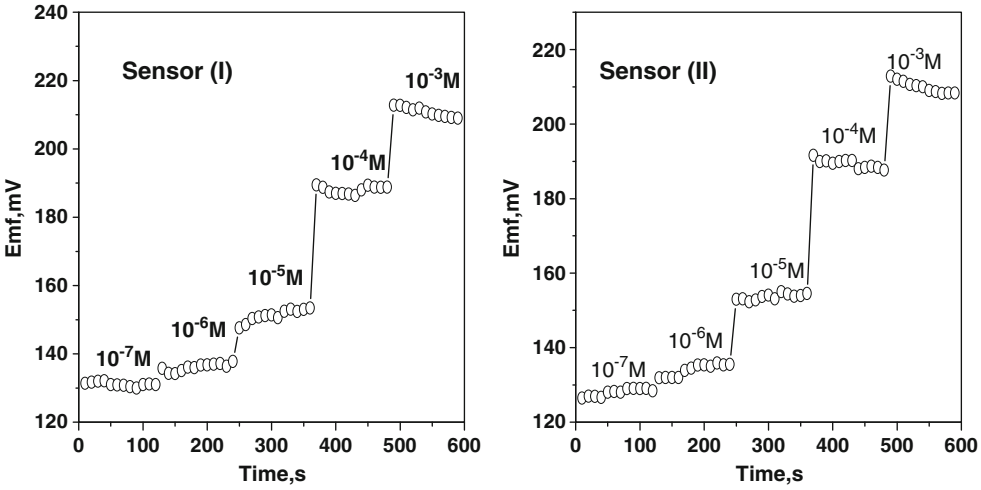

Fig. 3 Dynamic response times based membrane sensors towards different concentration levels of Pb(II)

the sensors with and without the anionic additive are presented in Table 1.

For checking the dependence of pH on the proposed sensors, potential-pH curves at various lead concentrations (10^{-3}–10^{-4} M) were constructed. For all sensors, the potentials were stable and practically unaffected by pH alterations over the working pH range 4.0–6.0 and 4.5–6.0 for sensors I and II, respectively (Table 1). Above pH 7, the potentials displayed by the electrode systems sharply decrease due to the precipitation of Pb^{2+} ions. At pH < 4, interferences from H^+ ions are significant with subsequent increasing in the potential response. All subsequent potentiometric measurements of lead ions were made in 10^{-2} M acetate buffer background of pH 5.0.

The dynamic time response for sensors based on ionophore (I) to reach ~95% of equilibrium response was ~20–30 s for 10^{-3}–10^{-5} M Pb(II) and ~10 s for $>10^{-6}$ M. Ionophore (II)-based membrane sensor reached its equilibrium response within 30 s for $>10^{-4}$ M Pb(II) and 10 s for $>10^{-5}$ M Pb(II). Potential stability was monitored over a period of 1 month to detect any change of the internal reference solution and its effect on the response. Response time for the proposed sensors is shown in Fig. 3.

Response of neutral carrier membranes

A simplest model of a neutral carrier membrane inserted between two electrolytic solutions is presented in Fig. 4. It is evident that lead ions are taken up by the membrane containing either ionophore (I) or (II). The distribution of Pb(II) ions (I^{+z}) between the outside solution and the respective complexes in the membrane can be fully characterized by overall distribution coefficients $K'_{i,n}$ and $K''_{i,n}$.

$$K'_{i,n} = k_{iCiL,n}(0)/C_i(0) = \beta_{\mathrm{is},n} k_i [C_L(0)]^n \quad (2)$$

$$K''_{i,n} = k_{iCiL,n}(d)/C_i(d) = \beta_{\mathrm{is},n} k_i [C_L(d)]^n \quad (3)$$

where $\beta_{iL,n}$ is the stability constant of the complex IL_n^{z+} in the membrane ($\beta_{is,0} = 1$), $C_{iL,n}$ is the concentration of the complex IL_n^{z+} in the membrane, and C_L is the concentration of the free ionophore L in the membrane. Apparently, the response of corresponding sensors towards lead ions, reflecting the relative mobilities or permeabilities of participating lead ion, forms over other ions present in the solution. Perm-selectivity for lead cation of the electroneutral membranes is predominant because the mobility of accompanying anions is very low as compared to the mobility of Pb(II) ions towards the organic membrane.

For neutral carrier-based sensors, introduction of ionic sites in the membrane bulk are not only necessary for obtaining Nernstian responses but also beneficial for various aspects, i.e., to improve the selectivity, to decrease the membrane resistance, and to reduce the interference from lipophilic counter-ions [49]. The enhancement of slope response and decrease in detection limit after addition of ionic sites in the membrane can be explained in which the ionophores exhibit strong affinity towards Pb^{2+} ions to create positively charged

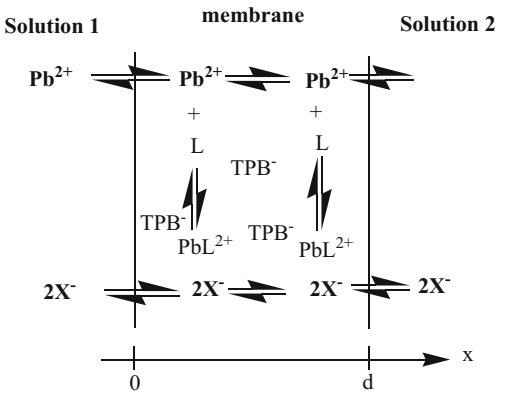

Fig. 4 Schematic representation of a neutral carrier polymeric lead membrane-based sensor

Table 2 Potentiometric selectivity coefficients (log*K*Pb2 + ,*j*) of lead membrane sensors

Interfere, *J*	log KPb2 + ,*j*			
	Ionophore (I)	Ionophore (II)	Ionophore (I) + TPB	Ionophore (II) + TPB
Zn^{2+}	−4.66	−4.29	−4.64	−4.01
Na^{+}	−7.58	−7.29	−7.61	−7.31
Li^{+}	−7.42	−6.75	−7.02	−6.80
Ca^{2+}	−4.30	−4.09	−4.21	−4.20
Ba^{2+}	−4.86	−4.38	−4.90	−4.44
Cu^{2+}	−5.20	−4.64	−5.01	−4.87
Ni^{2+}	−4.84	−4.22	−4.82	−4.33
Mg^{2+}	−4.54	−3.67	−4.61	−3.87
Cr^{3+}	−3.53	−2.81	−4.02	−2.93
Co^{2+}	−4.59	−3.88	−4.77	−4.01
Hg^{2+}	−4.54	−3.53	−4.11	−3.22
Fe^{2+}	−3.73	−3.95	−3.54	−3.65
Fe^{3+}	−2.11	−2.80	−2.32	−2.41

complexes in the membrane phase. These cationic complexes are stabilized by the presence of lipophilic anionic sites.

Potentiometric selectivity

Ionophores are important in controlling selectivity of membrane electrodes. Selectivity of membrane electrode is controlled by binding constant between ions and ionophore [50]. The selectivity coefficient of the sensors was defined by its relative response for the essential ion in presence other ions present in the solution [3]. The potentiometric selectivity coefficients ($K_{Pb}^{2+},_{B}^{Pot}$) of lead sensors were evaluated using the separate solution method (SSM) [51], using Eq. (4):

$$\text{Log } K = E_{\text{Pb}} - E_j/\text{slope} + \left[1 + Z_i/Z_j\right] \text{ log } \left[\text{Pb}^{2+}\right] \qquad (4)$$

where Z_j is the charge of the interfering ion and E_i, E_j are the potential values of Pb^{2+} and interfering ions, respectively. As shown in Table 2, the lead sensors based on ionophores (I) and (II) exhibit selectivity coefficients for Pb(II) ion over a large number of common cations. The selectivity order for ionophore (I) membrane-based sensor was as follows: Pb^{+2} > > Fe^{3+} > Cr^{3+} > Fe^{2+} > Ca^{2+} > Hg^{2+} = Mg^{2+} > Co^{2+} > Zn^{2+} > Ni^{2+} > Ba^{2+} > Cu^{2+} > Li^{+} > Na^{+}. For ionophore (II) membrane-based sensor, the selectivity order was as follows: Pb^{2+}> > Fe^{3+} ~ Cr^{3+} > Hg^{2+} > Mg^{2+} > Co^{2+} > Fe^{2+} > Ca^{2+} > Ni^{2+} ~ Zn^{2+} > Ba^{2+} > Cu^{2+} > Li^{+} > Na^{+}. For ionophore (I)-based membrane sensor doped with TPB^{-} as an anionic additive, the selectivity behavior of the sensor was in the following order: Pb^{+2}> > Fe^{3+} > Fe^{2+} > Cr^{3+} > Hg^{2+} > Ca^{2+} > Mg^{2+} > Zn^{2+} > Co^{2+} > Ni^{2+} > Ba^{2+} > Cu^{2+} > Li^{+} > Na^{+}. For ionophore (II)-based membrane sensor doped with TPB^{-} as an anionic additive, the selectivity behavior of the sensor was in the following order: Pb^{+2}> > Fe^{3+} > Cr^{3+} > Hg^{2+} > Fe^{2+} > Mg^{2+} > Zn^{2+} = Co^{2+} > Ca^{2+} > Ni^{2+} > Ba^{2+} > Cu^{2+} > Li^{+} > Na^{+}. This selectivity order indicates a preferred interaction between the

Table 3 Ionophore complex formation constants estimated using the segmented sandwich membranes method

Ion I^{+}	Formation constant log β_{ILn}	
	Ionophore I	Ionophore II
Pb^{2+}	11.5 ± 0.06	9.8 ± 0.12
Cu^{2+}	4.2 ± 0.03	4.15 ± 0.08
Zn^{2+}	4.3 ± 0.08	4.1 ± 0.01
Hg^{2+}	4.8 ± 0.06	5.4 ± 0.05
Fe^{3+}	7.3 ± 0.04	6.8 ± 0.03

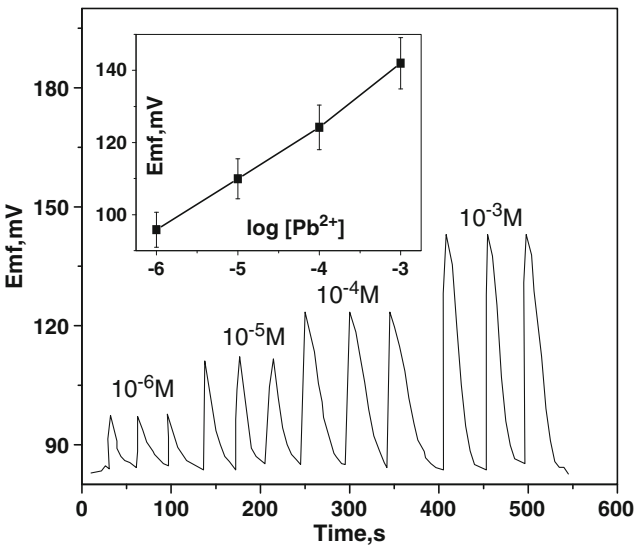

Fig. 5 Flow injection potentiometric responses obtained using ionophore (I) membrane-based sensor

Table 4 Response characteristic of ionophore (I) membrane-based sensor under FI operation

Parameter	Sensor I
Slope (mV/decade)[a]	15.3 ± 0.9
Correlation coefficient, *r*	0.999
detection limit (μg/mL)[a]	10^{-6}
Limit of linear range (M)	10^{-3}–10^{-6}
Optimum flow rate (mL/min)	5.0
Life span (week)	6
Response time (s)	<5
Output, sample/h	35~40

[a] Average of six measurements

proposed ionophores and Pb^{2+} ions as comparison with other cations. It could be noticed in Table 2 that lead sensors based on ionophore (I) exhibited better selectivity than those based on ionophore (II). This can be attributed to the presence of carboxylic group near from the -NH- group that could enhance the binding stability of the ionophore towards Pb^{2+} ions.

It is well established that the observed selectivity of polymeric membrane ISEs is greatly influenced by the formation constants of ion–ionophore complexes in the organic membrane phase. The segmented sandwich method [47] enables the estimation of ion–ionophore stability constants within the same PVC/plasticizer matrix employed to fabricate the ISE. The values of the formation constants (β) for most common heavy metals with the proposed ionophores in *o*-NPOE plasticized membranes are presented in Table 3.The data obtained of the formal stability constants agree well with the data of selectivity.

Flow injection

Flow-through analysis using potentiometric sensors showed high advantages such as low cost, simple instrumentation, and automation. In addition, the transient nature of the signal in flow injection analysis is help to overcome the effects of interfering ions if the electrode's response to the target analyte is faster than those interfering ions [52]. A tubular type detector incorporating ionophore (I) was prepared and used under hydrodynamic mode of operation for continuous Pb^{+2} quantification. A triplicate transient peaks were obtained from the flow injection analysis system under optimal experimental conditions and are shown in Fig. 5. A linear relationship between Pb^{+2} concentrations and FIA signals was obtained from a concentration range 1.0×10^{-6} to 1.0×10^{-3} M using 0.01 M acetate buffer, pH 5 as a carrier at a flow rate of 5 mL/min, with an injected volume 200 μL. The slope of the calibration plot under FIA mode was near-Nernstian (15.3 ± 1.9 mV/decade) with a detection limit 1.0×10^{-6} M. Table 4 shows the general response characteristics of sensor (I)-based PVC membrane detector under a flow-through mode of operation.

Analytical applications

Determination of Pb(II) in biological fluid

Application of the proposed method for quantification of lead in biological fluid was tested by spiking aliquots of serum samples with a known standard of lead in 1.0×10^{-2} M acetate buffer at pH 5. Results under the static mode of operation showed an average recovery of 95.6 and 94.7% with a relative standard deviation of 0.9 and 1.1% for ionophores (I) and (II) membrane-based sensors, respectively. Results obtained for determination of lead (II) in spiked human serum samples are listed in Table 5. The good agreement between the added and found lead content in the samples demonstrates the applicability of the sensor for routine analysis without a prior sample treatment.

Table 5 Determination of Pb(II) in biological samples using lead membrane-based sensor

Sample	Added, mol /L	Sensor I		Sensor II		Sensor I + TPB		Sensor II + TPB	
		Found, mol /L	Recovery, %	Found, mol /L	Recovery, %	Found, mol /L	Recovery, %	Found, mol /L	Recovery, %
Pb^{+2}	5.37×10^{-5}	5.12×10^{-5}	95.3	5.12×10^{-5}	95.3	5.27×10^{-5}	98.1	5.15×10^{-5}	95.9
	9.77×10^{-5}	9.26×10^{-5}	94.7	9.12×10^{-5}	93.3	9.57×10^{-5}	97.9	9.43×10^{-5}	96.5
	5.12×10^{-4}	4.89×10^{-4}	95.5	4.89×10^{-4}	95.5	5.11×10^{-4}	99.8	5.02×10^{-4}	98.0
	8.91×10^{-4}	8.51×10^{-4}	95.5	8.31×10^{-4}	93.2	8.88×10^{-4}	99.6	8.74×10^{-4}	98.1
	4.57×10^{-3}	4.46×10^{-3}	97.5	4.46×10^{-3}	97.5	4.37×10^{-3}	95.6	4.32×10^{-3}	94.5
	8.51×10^{-3}	8.12×10^{-3}	95.4	8.12×10^{-3}	95.4	8.21×10^{-3}	96.4	8.34×10^{-3}	98.0

Table 6 Performance features of some potentiometric lead membrane sensors based on neutral ionophores

Ionophore	Range, M	Slope, mV/decade	Detection limit, M	Interfering ion, log *K*	Ref.
Crown ether derivatives	1×10^{-6}–1×10^{-2}	30	25.5	Ag^+ (+0.17), Ni^{2+} (−1.36), La^{3+}, Fe^{3+}, Na^+, K^+	[35]
	$3 \times 10^{-0.6}$–2.5×10^{-3}	–	2×10^{-6}	Na^+, K^+, Li^+, Mg^{2+}, NH_4^+ (NR)	[36]
	1×10^{-6}–1×10^{-2}	58	$10^{-6.5}$	K^+, Tl^+, Ag^+, NH_4^+	[37]
Calixarene derivatives	1×10^{-6}–1×10^{-2}	30	6×10^{-7}	Ca^{2+}(−3.1), Cd^{2+}(−2.1), Zn^{2+}(−2.8), Co^{2+}(−2.8), Cu^{2+}(−2.3), Mg^{2+}(−3.3), Mn^{2+}(−3.1), Al^{3+}(−2.6), Fe^{3+}(−2.4), Cr^{3+}(−2.3), K^+(−2.2), Na^+(−2.5), Ag^+ (−2.0), Ni^{2+}(−2.2), Hg^{2+}(−1.5), Ba^{2+}(−3.9), Sr^{2+}(−3.7)	[32]
	1×10^{-6}–1×10^{-3}	25.5	1×10^{-6}	Na^+, K^+, Cu^{2+}, Ca^{2+}, Cd^{2+} (NR)	[38]
	1×10^{-5}–1×10^{-2}	29.5	1×10^{-6}	K^+(+0.36), Na^+(−1.04), Ag^+ (+16.31), Hg^{2+}(+3.26), Ca^{2+} (−1.1), Cu^{2+} (−0.74)	[39]
	1×10^{-5}–1×10^{-2}	28.0	1.4×10^{-6}	Th^{4+} (0.0), Sm^{3+} (−0.3), Ca^{2+} (−0.6), Dy^{3+} (−0.7), La^{3+} = Y^{3+} (−0.8), Ag^+ (−0.9), Cd^{2+} (−1.3), Zn^{2+} (−1.6), Mn^{2+} (−1.7), NH_4^+ (−2.2)	[40]
2,6 Bis pyridine--carboxamide derivatives	9×10^{-6}–1×10^{-2}	21.6	4.4×10^{-6}	Li^+ (−4.12), Na^+ (−3.70), K^+ (−4.11), Ca^{2+} (−1.91), Cu^{2+} (−1.99), Cd^{2+} (−1.94), Ag^+ (−2.89), Hg^{2+} (−1.5)	[41]
	5.8×10^{-5}–1×10^{-2}	33.1	1.8×10^{-5}	Li^+ (−3.40), Na^+ (−3.41), K^+ (−3.50), Ca^{2+} (−1.45), Cu^{2+} (−1.06), Cd^{2+} (−1.61), Ag^+(−2.89), Hg^{2+} (−1.00)	
	4×10^{-6}–1×10^{-2}	25.0	2.1×10^{-6}	Li^- (−3.83), Na^+ (−4.24), K^+ (−3.83), Ca^{2+} (−2.14), Cu^{2+}(−2.03), Cd^{2+} (−2.17), Ag^+ (−2.25), Hg^{2+} (−2.10)	
Schiff base derivatives	5.0×10^{-6}–0.1	29.4	2.0×10^{-6}	Ca^{2+} (−3.9), Cd^{2+} (−2.9), Zn^{2+} (−2.2), Co^{2+} (−3.1), Cu^{2+} (−2.8), Mg^{2+} (−3.1), Mn^{2+} (−2.9), Al^{3+} (−2.5), Fe^{3+} (−2.2), Cr^{3+} (−3.5), K^+ (−2.2), Na^+ (−2.3), NH_4^+ (−2.1), Ni^{2+} (−2.9)	[42]
	8×10^{-6}–1×10^{-1}	29.4	9×10^{-7}	Cu^{2+} (−2.7), Ba^{2+} (−3.1), Cd^{2+} (−3.6), Sr^{2+} (−3.8), Zn^{2+} (−4.1), Ca^{2+} (−4.1), Co^{2+} (−4.2), Mn^{2+} (−4.8), Mg^{2+} (−4..9), Na^+ (−2.5), K^+ (−2.2), Rb^+ (−2.5), Cs^+ (−2.6), Ag^+ (−2.2).	[43]
	5.0×10^{-6}–1.0×10^{-1}	28.9	5.0×10^{-6}	Ni^{2+} (−2.9), Cu^{2+} (−1.7), Cd^{2+} (−1.9), Cr^{3+} (−2.4), Hg^{2+} (−2.8), Zn^{2+} (−3.8), Co^{2+} (−2.6), Ca^{2+} (−3.6), Mg^{2+} (−2.4), Bi^{3+} (−3.6), Na^+ (−4.1), Sr^{2+} (−3.2), Al^{3+} (−2.7), Fe^{3+} (−2.6)	[44]
Dioxamide	1.3×10^{-2}–3.6×10^{-6}	29.7	2.0×10^{-6}	Ni^{2+} (−2.0), Co^{2+} (−3.4), Sr^{2+} (−2.4), Cu^{2+} (−2.2), Ba^{2+} (−1.6), Zn^{2+} (−2.1), Mg^{2+} (−2.8), Cd^{2+} (−2.4), Ca^{2+} (−2.3)	[45]
	1×10^{-6}–8.4×10^{-3}	31.9	NR	Hg^{2+} (−1.6), Fe^{2+} (−1.67), Cd^{2+} (−2.1)	[46]
Ionophore I	7×10^{-6}–1×10^{-3}	35.3	4.7×10^{-6}	Zn^{2+} (−4.66), Na^+ (−7.58), Li^+ (−7.42), Ca^{2+} (−4.3), Ba^{2+} (−4.86), Cu^{2+} (−5.2), Ni^{2+} (−4.84), Mg^{2+} (−4.54), Cr^{3+} (−3.53), Co^{2+} (−4.59), Hg^{2+} (−4.54), Fe^{2+} (−3.73), Fe^{3+} (−2.11)	This work
Ionophore I + TPB	1×10^{-6}–1×10^{-3}	39.4	8.0×10^{-7}	Zn^{2+} (−4.29), Na^+ (−7.29), Li^+ (−6.75), Ca^{2+} (−4.09), Ba^{2+} (−4.38), Cu^{2+} (−4.64), Ni^{2+} (−4.22), Mg^{2+} (−3.67), Cr^{3+} (−2.81), Co^{2+} (−3.88), Hg^{2+} (−3.53), Fe^{2+} (−3.95), Fe^{3+} (−2.80)	
Ionophore II	4×10^{-6}–1×10^{-3}	37.2	1.8×10^{-6}	Zn^{2+} (−4.64), Na^+ (−7.61), Li^+ (−7.02), Ca^{2+} (−4.21), Ba^{2+} (−4.90), Cu^{2+} (−5.01), Ni^{2+}(−4.82), Mg^{2+} (−4.61), Cr^{3+} (−4.02), Co^{2+} (−4.77), Hg^{2+} (−4.11), Fe^{2+} (−3.54), Fe^{3+} (−2.32)	
Ionophore II + TPB	5×10^{-6}–1×10^{-3}	43.9	6.0×10^{-7}	Zn^{2+} (−4.01), Na^+ (−7.31), Li^+ (−6.8), Ca^{2+} (−4.2), Ba^{2+} (−4.44), Cu^{2+} (−4.87), Ni^{2+} (−4.33), Mg^{2+} (−3.87), Cr^{3+} (−2.43), Co^{2+} (−4.01), Hg^{2+} (−3.22), Fe^{2+} (−3.65), Fe^{3+} (−2.41)	

NR not reported

Determination of Pb in alloy containing lead and tin

A certain weight of tin and lead alloy (0.04 g) with concentrated nitric acid, leaving a full day until completely dissolved and then complement to 100 mL of 10^{-2} M acetate buffer at pH 5. The lead (II) solution was measured by direct potentiometry using ionophore (I) and (II)-based membrane sensors. The results showed an average Pb content of 34.3 ± 0.2 (*w*/*w*) of the alloy. Similar results were obtained using atomic absorption spectrometry (i.e., 31.1 ± 0.5 *w*/*w*).

Conclusions

Novel synthetic quinoxaline derivatives ionophores are prepared, characterized, and used for construction of Pb(II) PVC

membrane sensors. The membrane sensors exhibited a wide linear concentration range of 4.0×10^{-6}–1.0×10^{-3} M and showed fast response times. Moreover, they exhibited enhanced response to wards Pb^{2+} ion over a wide range of other common heavy metal cations. A comparison with other lead sensors based on potentiometric transduction [32, 35–46] shown in Table 6 indicated better selectivity of the present sensors especially in the presence of Hg^{2+}, Cu^{2+}, Zn^{2+}, Cr^{3+}, Co^{2+}, Ni^{2+}, Fe^{2+}, and Fe^{3+} ions. The sensors are used for determining lead in biological fluids and in Pb/Sn alloys. Application of membrane electrodes was also applied for FIA monitoring of Pb^{+2} in different samples.

References

1. Clement RE, Yang PW, Koester CJ (1999) Environmental analysis. Anal Chem 71:257–292
2. Nriagu JO, Pacyna JM (1988) Quantitative assessment of worldwide contamination of air, water and soils by trace metals. Nature 333:134–139
3. Afkhami A, Shirzadmehr A, Madrakian T, Bagheri H (2014) Improvement in the performance of a Pb^{2+} selective potentiometric sensor using modified core/shell SiO_2/Fe_3O_4 nano-structure. J Mol Liq 199:108–114
4. Baird C, Cann M (2005) Environmental chemistry. Freeman and Company, New York
5. Papanikolaou NC, Hatzidaki EG, Belivanis S, Tzanakakis GN, Tsatsakis AM (2005) Lead toxicity update. A brief review. Med Sci Monit 11:329–336
6. Zimkus A, Cretscu I, Grzybowska I, Radecka H, Geise HJ, Dieltiens P, Aleksandrzak K (2003) Potentiometric lead (II) ions recognition by liquid membrane electrodes incorporating methoxy substituted arylenevinylene derivatives. Pol J Env Studies 6:773–778
7. De Smaelea T, Moens L, Dams R, Sandra P, Van der Eycken J, Vandyck J (1998) Sodium tetra (*n*-propyl) borate: a novel aqueous in situ derivatization reagent for the simultaneous determination of organomercury, lead and tin compounds with capillary gas chromatography–inductively coupled plasma mass spectrometry. J Chromatogr A 793:99–106
8. Centineo G, González EB, Sanz-Medel A (2004) Multi elemental speciation analysis of organometallic compounds of mercury, lead and tin in natural water samples by headspace-solid phase microextraction followed by gas chromatography–mass spectrometry. J Chromatogr A 1034:191–197
9. Ceulemans M, Adams FC (1996) Integrated sample preparation and speciation analysis for the simultaneous determination of methylated species of tin, lead and mercury in water by purge-and-trap injection-capillary gas chromatography-atomic emission spectrometry. J Anal Atomic Spec 11:201–206
10. Moens L, De Smaele T, Dams R (1997) Sensitive, simultaneous determination of organomercury, lead and tin compounds with headspace solid phase microextraction capillary gas chromatography combined with inductively coupled plasma mass spectrometry. Anal Chem 69:1604–1611
11. Pereiro R, Díaz AC (2002) Speciation of mercury, tin, and lead compounds by gas chromatography with microwave-induced plasma and atomic emission detection (GC–MIP–AED). Anal Bioanal Chem 372:74–90
12. Hu Q, Yang G, Zhao Y, Yin J (2003) Determination of copper, nickel, cobalt, silver, lead, cadmium, and mercury ions in water by solid-phase extraction and the RP-HPLC with UV-Vis detection. Anal Bioanal Chem 375:831–835
13. Barałkiewicz D, Kozka M, Piechalak A, Tomaszewska B, Sobczak P (2009) Determination of cadmium and lead species and phytochelatins in pea (*Pisum sativum*) by HPLC–ICP-MS and HPLC–ESI-MSn. Talanta 79:493–498
14. Hu Q, Yang G, Yin J, Yao Y (2002) Determination of trace lead, cadmium and mercury by on-line column enrichment followed by RP-HPLC as metal-tetra-(4-bromophenyl)-porphyrin chelates. Talanta 57:751–756
15. Wang L, Hu Q, Guangyu Y, Yin J, Yuan Z (2003) Determination of lead, cadmium, and mercury by on-line enrichment followed by RP-HPLC. J Anal Chem 58:1054–1059
16. Feng R, Machado N, Ludden J (1993) Lead geochronology of zircon by laser probe-inductively coupled plasma mass spectrometry (LP-ICPMS). Geochim Cosmochim Acta 57:3479–3486
17. Walder AJ, Abell ID, Platzner I (1993) Lead isotope ratio measurement of NIST 610 glass by laser ablation inductively coupled plasma mass spectrometry. Spectrochim Acta 488:397–402
18. Nixon DE, Moyer TP (1996) Routine clinical determination of lead, arsenic, cadmium, and thallium in urine and whole blood by inductively coupled plasma mass spectrometry. Spectrochim Acta B 51: 13–25
19. Schramel P, Wendler I, Angerer J (1997) The determination of metals (antimony, bismuth, lead, cadmium, mercury, palladium, platinum, tellurium, thallium, tin and tungsten) in urine samples by inductively coupled plasma-mass spectrometry. Int Arch Occup Environ Health 69:219–223
20. Bhandari SA, Amarasiriwardena D (2000) Closed-vessel microwave acid digestion of commercial maple syrup for the determination of lead and seven other trace elements by inductively coupled plasma-mass spectrometry. Microchim J 64:73–84
21. Stoeppler M, Brandt K (1978) Contributions to automated trace analysis. Part II. Rapid method for the automated determination of lead in whole blood by electrothermal atomic-absorption spectrophotometry. Analyst 103:714–722
22. Li Z, Tang J, Pan J (2004) The determination of lead in preserved food by spectrophotometry with dibromo hydroxyl phenyl porphyrin. Food Control 15:565–570
23. Shockravi A, Chaloosi M, Rostami E, Heidaryan D, Shirzadmehr A, Fattahi H, Khoshsafar H (2007) Modified BINOL Podands: synthesis of dinaphthosulfide podands and their application in spectrophotometric determination of toxic metals. Phosphorus Sulfur Silicon 182:2115–2123
24. El-Naby EH, Kamel AH (2015) Potential transducers based mantailored biomimetic sensors for selective recognition of dextromethorphan as an antitussive drug. Mat Sci Eng C 54:217–224
25. Kamel AH (2015) Potentiometric transducer based on a Mn(II) [2 formylquinoline thiosemicarbazone] complex for static and hydrodynamic assessment of azides. Talanta 144:1085–1090
26. Kamel AH, Argig AAA (2017) Automatic potentiometric system for quantification of three imidazole derivatives based on new polymeric PVC membrane sensors. Ionics Online 7 March, DOI: 10.1007/s11581-017-2029-6.
27. Kamel AH, Hassan AME (2016) Solid contact potentiometric sensors based on host-tailored molecularly imprinted polymers for creatine assessment. Int J Electrochem Sci 11:8938–8949
28. Hassan SSM, Kamel AH, Abd El-Naby H (2014) Novel potentiometric sensors for batch and continuous monitoring of alizarin red S dye and their application for aluminum assessment. J Chin Chem Soc 61:295–302
29. Li M, Zhou H, Shi L, Li D, Long Y (2014) Ion-selective gold–thiol film on integrated screen printed electrodes for analysis of Cu (II) ions. Analyst 139:643–648

30. Kamel AH (2007) A novel flow-through planar solid contact sensor for the determination of lead with potentiometric anionic response. Electroanalysis 19:2419–2427
31. Frant MS (1994) History of the early commercialization of ion-selective electrodes. Analyst 119:2293–2301
32. Bhat VS, Ijeri VS, Srivastava AK (2004) Coated wire lead (II) selective potentiometric sensor based on 4-*tert* butylcalix[6]arene. Sens Actu B 99:98–105
33. Buhlmann P, Pretsch E, Bakker E (1998) Carrier-based ion-selective electrodes and bulk optodes. 2. Ionophores for potentiometric and optical sensors. Chem Rev 98:1593–1688
34. Guziński M, Lisak G, Kupis J, Jasiński A, Bocheńska M (2013) Lead (II)-selective ionophores for ion-selective electrodes: a review. Anal Chim Acta 791:1–12
35. Mousavi MF, Sahari S, Alizadeh N, Shamsipur M (2000) Lead ion-selective membrane electrode based on 1,10-dibenzyl-1,10-diaza-18-crown-6. Anal Chim Acta 414:189–194
36. Davini E, Mazzamurro G, Piotto AP (1992) Lead-selective FET: complexation selectivity of ionophores embedded in the membrane. Sens. Actuat. B. 7:580–583
37. Hasse W, Ahlers B, Reinbold J, Cammann K (1994) $PbOH^+$ selective membrane electrode based on crown ethers. Sens Actuat B 19: 383–386
38. Wroblewski W, Brzozka Z (1996) Switching of ion selectivity of membranes by lipophilic ionic sites. Anal Chim Acta 326:163–168
39. Cadogan F, Kan P, McKervey MA, Diamond D (1999) Lead-selective electrodes based on calixarene phosphine oxide derivatives. Anal Chem 71:5544–5550
40. Yaftian MR, Rayati S, Emadi D, Matt D (2006) A coated wire-type lead (II) ion-selective electrode based on a phosphorylated calix[4]arene derivative. Anal Sci 22:1075–1078
41. Hassan SSM, Abou Ghalia MH, Amr AE, Mohamed AHK (2003) New lead (II) selective membrane potentiometric sensors based on chiral 2,6-bis pyridinecarboximide derivatives. Talanta 60:81–91
42. Ardakany MM, Ensafi AA, Naeimi H, Dastanpour A, Shamlli A (2003) Highly selective lead (II) coated-wire electrode based on a new Schiff base. Sens. Actuat. B 96:441–445
43. Jeong T, Lee HK, Jeong D, Jeon S (2005) A lead (II)-selective PVC membrane based on a Schiff base complex of *N*,*N*'-bis(salicylidene)-2,6-pyridinediamine. Talanta 65:543–548
44. Mazlum M, Kashani MK, Salavati-Niasari M, Ensafi AA (2005) Lead ion-selective electrode prepared by sol–gel and PVC membrane techniques. Sens. Actuat. B 107:438–445
45. Kazemi SY, Shamsipur M, Sharghi H (2009) Lead-selective poly (vinyl chloride) electrodes based on some synthesized benzo-substituted macrocyclic diamides. J Hazard Mat 172:68–73
46. Borraccino A, Campanella L, Sammartino MP, Tomassetti M, Battilotti M (1992) Suitable ion-selective sensors for lead and cadmium analysis. Sens Actuat B 7:535–539
47. Mi Y, Bakker E, Pretsch E (1999) Determination of complex formation constants of lipophilic neutral ionophores in solvent polymeric membranes with segmented sandwich membranes. Anal Chem 71:5279–5287
48. Linder E, Umezawa Y (2008) Performance evaluation criteria for preparation and measurement of macro- and micro-fabricated ion-selective electrodes (IUPAC Technical Report). Pure Appl Chem 80:85–104
49. Bakker E, Pretsch E, Buhlmann P (2000) Selectivity of potentiometric ion sensors. Anal Chem 72:1127–1133
50. Buck RP, Sandifer JR (1973) Mixed divalent, univalent cation responses of completely ionized liquid membrane systems. J Phys Chem 77:2122–2128
51. Umezawa Y, Buhlmann P, Umezawa K, Tohda K, Amemiya S (2000) Potentiometric selectivity coefficients of ion-selective electrodes. Part I. Inorganic cations (technical report). Pure Appl Chem 72:1851–2082
52. Cammann K (1988) Flow injection analysis with electrochemical detection. Fres Z Anal Chem 329:691–697